Comparison of the Diagnostic Performance of Four Quantitative Myocardial Perfusion Estimation Methods Used in Cardiac MR Imaging: CE-MARC Substudy[1]

John D. Biglands, PhD
Derek R. Magee, PhD
Steven P. Sourbron, PhD
Sven Plein, PhD
John P. Greenwood, PhD
Aleksandra Radjenovic, PhD

Purpose: To compare the diagnostic performance of four tracer kinetic analysis methods to quantify myocardial perfusion from magnetic resonance (MR) imaging cardiac perfusion data sets in terms of their ability to lead to the diagnosis of myocardial ischemia.

Materials and Methods: The study was approved by the regional ethics committee, and all patients gave written consent. A representative sample of 50 patients with suspected ischemic heart disease was retrospectively selected from the Clinical Evaluation of Magnetic Resonance Imaging in Coronary Heart Disease trial data set. Quantitative myocardial blood flow (MBF) was estimated from rest and adenosine stress MR imaging perfusion data sets by using four established methods. A matching diagnosis of both an inducible defect as assessed with single photon emission computed tomography and a luminal stenosis of 70% or more as assessed with quantitative x-ray angiography was used as the reference standard for the presence of myocardial ischemia. Diagnostic performance was evaluated with receiver operating characteristic (ROC) curve analysis for each method, with stress MBF and myocardial perfusion reserve (MPR) serving as continuous measures.

Results: Area under the ROC curve with stress MBF and MPR as the outcome measures, respectively, was 0.86 and 0.92 for the Fermi model, 0.85 and 0.87 for the uptake model, 0.85 and 0.80 for the one-compartment model, and 0.87 and 0.87 for model-independent deconvolution. There was no significant difference between any of the models or between MBF and MPR, except that the Fermi model outperformed the one-compartment model if MPR was used as the outcome measure ($P = .02$).

Conclusion: Diagnostic performance of quantitative myocardial perfusion estimates is not affected by the tracer kinetic analysis method used.

Online supplemental material is available for this article.

[1] From the Division of Medical Physics (J.D.B., S.P.S.) and Division of Cardiovascular and Diabetes Research (S.P. J.P.G.), Leeds Institute of Cardiovascular and Metabolic Medicine, University of Leeds, Worsley Building, Leeds LS2 9JT, England; Department of Medical Physics and Engineering, Leeds Teaching Hospitals NHS Trust, Leeds, England (J.D.B.); School of Computing, University of Leeds, Leeds, England (D.R.M.); and Institute of Cardiovascular and Medical Sciences, College of Medical, Veterinary and Life Sciences, University of Glasgow, Glasgow, Scotland (A.R.). Received February 20, 2014; revision requested April 14; revision received July 28; accepted August 8; final version accepted October 3. J.D.B. supported by an NIHR research training fellowship (NIHR/RTF/01/08/014). S.P. supported by a British Heart Foundation fellowship (FS/10/62/28409). S.P. and J.P.G. supported by an educational research grant from Philips Healthcare. D.R.M. and A.R. supported in part by WELMEC, a Centre of Excellence in Medical Engineering funded by the Wellcome Trust and EPSRC, under grant number WT 088908/Z/09/Z. **Address correspondence to** J.D.B. (e-mail: *jdb@medphysics.leeds.ac.uk*).

The views expressed in this publication are those of the authors and not necessarily those of the NHS, the National Institute for Health Research, or the Department of Health.

Dynamic contrast material–enhanced (DCE) magnetic resonance (MR) imaging cardiac perfusion is one of several imaging techniques, including positron emission tomography (PET) and single photon emission computed tomography (SPECT), that have been shown to be useful in the noninvasive diagnosis of myocardial ischemia (1). To generate quantitative estimates of myocardial blood flow (MBF), a variety of tracer kinetic analysis methods have been devised and validated in animal (2,3) and human (4,5) studies. Quantitative MBF estimates have the potential to play an important role in the diagnosis of ischemic heart disease by increasing objectivity (6–8) and potentially improving diagnostic sensitivity over visual analysis, especially in the presence of multivessel disease (9). However, there is a large variation in published perfusion estimates between studies (4,10). This could be due to differences in patient population, contrast agent injection protocol, imaging pulse sequence, and tracer kinetic analysis methods. Investigations into differences between tracer kinetic methods have been performed previously (11,12). However, the effect of these differences on the diagnosis of ischemic heart disease has not been studied.

Given the null hypothesis that no difference exists between the MBF estimates generated with different methods, the purpose of this study was to compare the diagnostic performance of four tracer kinetic analysis methods in the quantification of myocardial perfusion from MR imaging cardiac perfusion data sets in terms of their ability to aid in the diagnosis of myocardial ischemia. The selected models were chosen to represent the most commonly used methods appropriate for use in the heart; thus, we used Fermi-constrained deconvolution (6,8,9,13), model-independent deconvolution (14,15), a one-compartment model (16,17), and an uptake model (12,18–20).

Advances in Knowledge

- Myocardial blood flow (MBF) estimates obtained with four tracer kinetic analysis methods correlate well with each other ($R \geq 0.88$) but show significant differences in mean values (analysis of variance, $P < .01$).
- There is no significant difference between the four methods in the ability to diagnose ischemic heart disease when the stress MBF is used ($P \geq .26$); when myocardial perfusion reserve (MPR) is used, the one-compartment model underperforms compared with the Fermi-constrained deconvolution technique ($P = .02$).
- Division of stress MBF values by the rest measurement to calculate MPR does not improve diagnostic accuracy ($P \geq .29$).

Materials and Methods

Study Population

The study protocol was approved by the regional research ethics committee. A subset of 50 patients who had been consecutively recruited for the Clinical Evaluation of Magnetic Resonance Imaging in Coronary Heart Disease (or CE-MARC) trial with suspected angina pectoris were selected. The subset was selected such that the distribution of risk factors (hypertension, diabetes, smoking, age) and disease status (healthy or single-, double-, or triple-vessel disease) was representative of those in the full Clinical Evaluation of Magnetic Resonance Imaging in Coronary Heart Disease population. The reference standard was constructed from the matching diagnosis of x-ray angiography (quantitative coronary angiography [QCA]) and SPECT imaging. Cases with an angiographic QCA lesion stenosis of 70% or more and a positive (inducible defect) SPECT report were classified as ischemic, and patients with no QCA lesion stenosis of more than 50% and a normal SPECT report were classified as nonischemic (normal). Patients with angiographic QCA stenoses between 50% and 70% or with discordant angiographic and SPECT results were not included in the study.

Imaging

SPECT images, myocardial perfusion MR images, and QCA data were acquired from each patient, as described previously (21,22). Adenosine-induced stress imaging was performed 15 minutes before rest imaging. Myocardial perfusion MR imaging was performed by using bolus intravenous injection of 0.05 mmol per kilogram of body weight gadopentetate dimeglumine (Magnevist; Schering, West Sussex, England). Images were acquired by using a

Implications for Patient Care

- There is no evidence to show that, of the methods compared in this study, the tracer kinetic analysis method used in quantitative cardiac perfusion affects diagnostic performance.
- When data are to be interpreted in terms of quantitative MBF values, it may be possible to discard rest imaging from the investigation with no loss of diagnostic power.

Published online before print
10.1148/radiol.14140433 **Content code:** CA

Radiology 2015; 275:393–402

Abbreviations:
AHA = American Heart Association
AUC = area under the ROC curve
DCE = dynamic contrast material enhanced
MBF = myocardial blood flow
MPR = myocardial perfusion reserve
QCA = quantitative coronary angiography
ROC = receiver operating characteristic

Author contributions:
Guarantors of integrity of entire study, J.D.B., S.P., A.R.; study concepts/study design or data acquisition or data analysis/interpretation, all authors; manuscript drafting or manuscript revision for important intellectual content, all authors; approval of final version of submitted manuscript, all authors; agrees to ensure any questions related to the work are appropriately resolved, all authors; literature research, J.D.B., A.R.; clinical studies, S.P.S., S.P., J.P.G., A.R.; experimental studies, J.D.B.; statistical analysis, J.D.B., D.R.M., S.P.S., A.R.; and manuscript editing, all authors

Funding:
This research was supported by the Wellcome Trust (grant number WT 088908/Z/09/Z).

Conflicts of interest are listed at the end of this article.

T1-weighted saturation recovery turbo field-echo imaging sequence. A shared (non–section-selective) saturation pulse was used, giving prepulse delay times of 126 msec, 272 msec, and 418 msec for the basal, middle, and apical sections, respectively. The pulse sequence parameters were as follows: repetition time msec/echo time msec, 2.7/1.0; flip angle, 15°, sensitivity encoding factor, 2; matrix, 144 × 144; field of view, 320–460 mm; section thickness, 10 mm; and partial Fourier factor, 0.67.

Contouring

Contouring, subsequent quantitative analysis, and statistical analysis were performed by a medical physicist (J.D.B.) with more than 10 years of MR imaging experience. Contours depicting the myocardium and a region within the left ventricular blood pool were drawn by using dedicated cardiac image analysis software (Mass 7.0; Medis, Leiden University, Leiden, the Netherlands) (Fig 1). These contours were copied to all time frames and manually adjusted for breathing motion by using rigid translation. The myocardium was subdivided into six circumferentially equidistant regions in the basal and middle sections and four in the apical section according to the standard Amercan Heart Association (AHA) model (23).

Exclusions

Individual perfusion data sets exhibiting excessive (more than one frame) through-plane motion (typically due to electrocardiographic gating failure) were visually identified and were excluded prior to MBF quantitation. To exclude thin myocardial segments, which are prone to partial volume errors and low signal-to-noise ratio, segments with a myocardial width of less than 1 voxel at the acquisition resolution were excluded.

Concentration Conversion

The method used to generate contrast agent concentration curves is described in Appendix E1 (online). All precontrast signal estimates (S_0) were taken from the stress study. Values of 1435 msec and 4.3 $sec^{-1} \cdot mmol/L^{-1}$ were used for blood T1 and contrast agent relaxivity, respectively. After concentration conversion, baseline subtraction of the rest curves was performed to remove the contribution of any remnant contrast agent.

Preprocessing

The arterial input function was taken from the basal section. The precontrast time period of the curves was identified by fitting a piecewise linear-linear function to the data and identifying the first linear component as the baseline (24). To correct for the time shift, *dt*, between the onset of contrast agent in the arterial input function and the myocardium, the tracer kinetic model was fitted to the data multiple times over a range of values (zero to five times the temporal resolution at acquisition). The delay time yielding the optimal χ^2 fit to the data was used in the analysis. All curves were interpolated by a factor of four by using a piecewise cubic hermite interpolating polynomial (25), termed *pchip* (Matlab; Mathworks, Natick, Mass), prior to analysis to allow for *dt* values less than the temporal resolution at acquisition. Model fitting was performed by using the Levenberg-Marqurdt algorithm, termed *lsqcurvefit* (Mathworks). Model-independent deconvolution analysis did not require correction for *dt* and was solved by using singular value decomposition with Tikhonov regularization (15).

For Fermi-constrained deconvolution, only the sections of the curve corresponding to the first pass of contrast agent through the heart were used in the analysis. The end of the first-pass cutoff point was found automatically, as described previously (26). The uptake model is only valid in the early phases after contrast agent arrival, so the time point corresponding to the peak of the arterial input function was taken as the cutoff point (12). Figure 1 shows the different cutoff points and corresponding fits for each of the four methods.

Quantitative Myocardial Blood Flow Estimation

The four tracer kinetic analysis methods used to estimate MBF are described in detail in Appendix E2 (online). Briefly, Fermi-constrained deconvolution (13) uses a three-parameter Fermi function to constrain the impulse response function. Model-independent deconvolution (14,15) avoids such constraints, although appropriate regularization is necessary. The one-compartment model (16,17,27) assumes that the myocardium is flow limited, meaning that the permeability between the vascular and extracellular spaces is sufficiently high and that the two spaces act as one compartment. The uptake model (12,18–20) makes the further assumption that at early time points, venous output concentration is zero, reducing the analysis to a straight line fit.

Computing a Diagnosis

The diagnosis in question was that of ischemic heart disease, as assessed with cardiac MR imaging. The reference standard measurement was the matching diagnosis of an inducible defect at SPECT and a coronary artery stenosis of 70% or more at QCA. Diagnosis was made on a per-patient basis rather than on a per-vessel basis (ie, no account was taken of whether the myocardial segment exhibiting a perfusion defect was supplied by the diseased coronary artery according to the AHA mapping). To compute a diagnosis from the MR imaging data, each analysis method was applied to each of the 16 segments of the AHA model, both at rest and at stress, in all of the patients. Myocardial perfusion reserve (MPR) values were calculated as the stress MBF estimate divided by the resting MBF estimate. The minimum MPR or stress MBF measurement from all AHA segments in a given patient was taken as the one diagnostic measurement from quantitative MR imaging. Diagnostic performance was evaluated by using receiver operating characteristic (ROC) curve analysis, taking the agreed diagnosis between SPECT and QCA as the reference standard. Separate ROC curves were generated by using MPR and stress MBF values for each tracer kinetic analysis method.

Figure 1

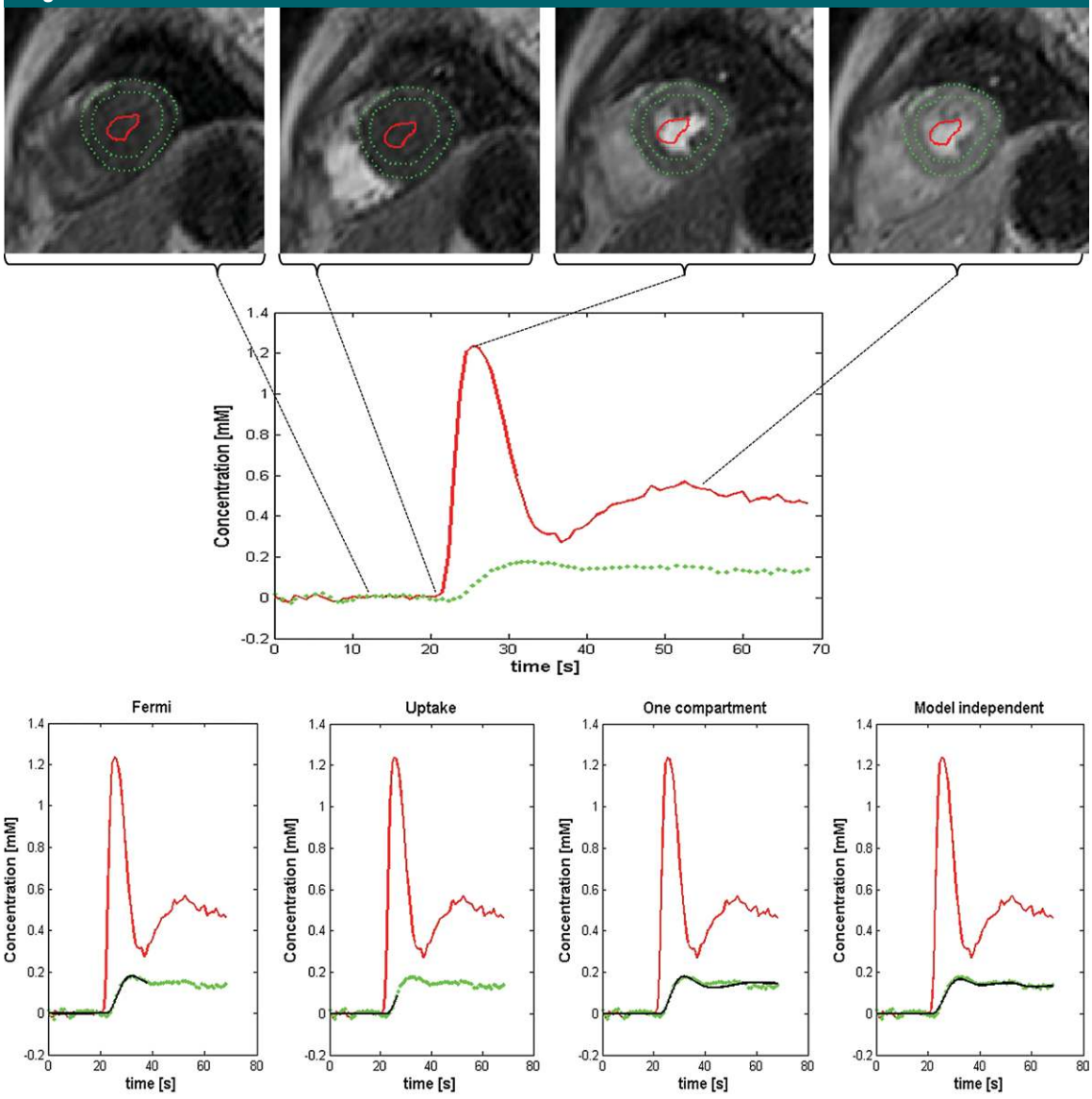

Figure 1: Analysis methodology. Contours are drawn around the myocardium (dashed line) and within the left ventricular blood pool (solid line) to generate concentration versus time curves for the myocardium and arterial input function, respectively. Lower plots show resulting concentration versus time plots. The model fits are shown as a solid black line extending over only the portion of the curve used for that model. The Fermi model is limited to the first pass, and the uptake model is limited to the peak of the arterial input function. The one-compartment model and the model-independent method fit to the whole data set.

Statistical Analysis

Statistical analysis was performed by using statistical software (SPSS, version 21.0, SPSS, Chicago, Ill; Analyse-it, Analyse-it Software, Leeds, England). To test for differences between perfusion estimates, analysis of variance was used with a pairwise Tukey test to determine which methods were different. The Pearson correlation coefficient was calculated to test for correlation between methods. Bland-Altman plots were used to show agreement between the different methods, and mean biases were calculated. ROC curves were generated by using MPR or stress MBF as the continuous measure. The area under the ROC curve (AUC) was calculated for each ROC curve. The optimal perfusion metric cutoff value for the ROC curve was taken as the point where the true-positive and true-negative lines crossed on the decision plot. A DeLong et al nonparametric AUC comparison (28) was used to compare the diagnostic performance of the different methods.

Results

The study consisted of 50 patients (mean age, 59 years; age range, 40–77 years), 32 of whom were men (mean age, 59 years; age range, 45–75 years) and 18 of whom were women (mean age, 60 years; age range, 40–77 years). There was no significant age difference between the men and women (P = .71). This population comprised 31 patients without ischemia and 19 patients with ischemia, 12 of whom had single-vessel disease, six of whom had double-vessel disease, and one who had triple-vessel disease. There were no occluded vessels in this subpopulation, with all patients having normal antegrade coronary flow (TIMI III). Analysis of late gadolinium enhancement images showed that eight patients had evidence of myocardial scarring (infarct pattern). Two perfusion data sets (one at rest and one at stress) (2%) were excluded from the study because of severe through-plane motion caused by electrocardiographic triggering failures. A total of 71 (4.5%) AHA segments were shown to have a myocardial width of less than 1 voxel and were excluded. The majority of these exclusions were in the basal, more diastolic, section. Seven of the excluded segments corresponded to myocardial infarction, as assessed with the late gadolinium enhancement images. Table E1 (online) provides a breakdown of the section position and rest or stress status of exclusions.

The quantitative results for each model, grouped into patients with and those without ischemia, are shown in Table 1. There was a significant difference between nonischemic and ischemic measurements for stress MBF (P < .001) and MPR (P < .001) values but not for rest MBF values (P = .97).

Bland-Altman agreement plots for each of the models are shown in Figure E1 (online). Both rest and stress MBF measurements are included in the comparisons. Table 2 shows the results of the comparisons between the models. Combined stress and rest average MBF measurements were significantly different between the methods (analysis of variance, P < .01). A post hoc Tukey test showed that these differences were significant between all methods, except for the comparison between the Fermi model and the one-compartment model. These observations were maintained when stress and rest MBFs were considered separately. MPR measurements were also significantly different (analysis of variance, P = .04), and the Tukey test revealed that this was due to a significant difference between the Fermi method and the model-independent method. Comparisons between the other models did not exhibit significant differences. The Bland-Altman assessment showed that the maximum difference between models was 0.48 mL/g/min for MBF measurement and 0.18 for MPR measurement.

When individual coronary territories as defined by the AHA myocardial segmentation model (23) were considered, MPR-based ROC curve AUC values in the left circumflex, left anterior descending, and right coronary arteries were 0.65 (95% confidence interval: 0.39, 0.90), 0.94 (95% confidence interval: 0.87, 1.0), and 0.74 (95% confidence interval: 0.47, 1.0), respectively. When single-vessel disease and multivessel disease were considered separately, the AUC values were 0.92 (95% confidence interval: 0.83, 1.0) and 0.94 (95% confidence interval: 0.86, 1.0), respectively. These vessel-specific analyses were performed by using the MBF values obtained with the Fermi model. In 13 (63%) of 19 cases, the minimum perfusion score corresponded to a coronary artery territory that contained a significant stenosis according to the AHA segmentation model.

ROC curves for each of the models are shown in Figure 2. Both the stress MBF curve and the MPR curve are shown. Table 3 shows the AUC, optimal ROC cutoff perfusion score, and test sensitivity and specificity at that cutoff value. Table 2 shows the DeLong et al comparison scores between the ROC curves from the four models. There were no significant differences in diagnostic performance between the models when stress MBF values were used. When using MPR values, the one-compartment model performed significantly worse than the Fermi model, but no significant differences were found between the other models. The stress MBF and MPR ROC curves are directly compared in Figure 3. No significant differences were found between stress MBF and MPR diagnostic curves with any of the analysis methods.

Table 1

MBF and MPR Measurements in Patients with and Those without Ischemia over All AHA Segments from the Four Models

Measurement	Fermi Method	Uptake Method	One-Compartment Model	Model-independent Deconvolution
Stress MBF (mL/min/g)				
Patients without ischemia	3.18 ± 1.38	2.77 ± 1.22	3.01 ± 1.29	2.35 ± 1.26
Patients with ischemia	2.24 ± 1.02	1.99 ± 0.91	2.29 ± 0.93	1.68 ± 0.77
Rest MBF (mL/min/g)				
Patients without ischemia	1.28 ± 0.54	1.20 ± 0.58	1.32 ± 0.56	1.01 ± 0.42
Patients with ischemia	1.28 ± 0.63	1.17 ± 0.63	1.36 ± 0.56	1.01 ± 0.47
MPR				
Patients without ischemia	2.59 ± 1.02	2.51 ± 1.22	2.43 ± 1.31	2.39 ± 1.01
Patients with ischemia	1.92 ± 0.93	1.90 ± 0.94	1.88 ± 1.11	1.78 ± 0.67

Note.—Data are mean ± standard deviation.

Discussion

This study has shown that the diagnostic performance of quantitative perfusion measurements is not affected by

Table 2

Statistical Comparisons between the Four Models

Statistic	Fermi vs Uptake	Fermi vs One-Compartment Model	Fermi vs Model-independent Deconvolution	Uptake vs One-Compartment Model	Uptake vs Model-independent Deconvolution	One-Compartment Model vs Model-independent Deconvolution
Pearson *r* statistic						
MBF	0.97	0.94	0.91	0.91	0.88	0.92
Bland Altman bias						
Stress MBF	−0.35 (−1.05, 0.34)	−0.07 (−1.09, 0.54)	−0.69 (−1.94, 0.54)	0.27 (−0.85, 1.40)	−0.35 (−1.58, 0.88)	−0.62 (−1.70, 0.46)
Rest MBF	−0.09 (−0.65, 0.47)	0.06 (−0.47, 0.60)	−0.26 (−0.86, 0.34)	0.15 (−0.60, 0.91)	−0.17 (-0.93, 0.59)	−0.32 (−0.93, 0.29)
MBF	−0.22 (−0.90, 0.46)	−0.01 (−0.83, 0.82)	−0.48 (−1.55, 0.59)	0.21 (−0.75, 1.18)	−0.26 (−1.30, 0.78)	−0.47 (−1.40, 0.45)
MPR	−0.05 (−1.38, 1.28)	−0.12 (−2.06, 1.83)	−0.18 (−1.64, 1.29)	−0.07 (−2.03, 1.90)	−0.12 (−2.08, 1.83)	−0.06 (−2.10, 1.99)
Tukey *t* test *P* value						
MBF	<0.01	0.99	<0.01	<0.01	<0.01	<0.01
MPR	0.75	0.11	0.04	0.58	0.08	0.67
P value for comparison of ROC curves between methods						
Stress MBF	0.39	0.51	0.84	0.99	0.50	0.26
MPR	0.13	0.02	0.17	0.24	0.99	0.18
Difference in AUC between methods						
Stress MBF	0.02 (−0.02, 0.05)	0.02 (−0.03, 0.06)	−0.01 (−0.06, 0.05)	0.00 (−0.05, 0.05)	−0.02 (−0.08, 0.04)	−0.02 (−0.06, 0.02)
MPR	0.05 (−0.01, 0.11)	0.12 (0.02, 0.21)	0.05 (−0.02, 0.12)	−0.07 (−0.18, 0.05)	0.00 (−0.10, 0.1)	−0.07 (−0.16, 0.03)

Note.—Data in parentheses are 95% confidence intervals.

the choice of tracer kinetic analysis method when stress MBF measurements are used. This suggests that any of the methods can be used with equal confidence for diagnosis of myocardial ischemia. In addition, the results show that normalization of stress MBF values by resting MBF values to generate MPRs does not significantly improve diagnostic performance, suggesting that rest perfusion measurements may not be necessary when quantitative perfusion estimates are used to diagnose myocardial ischemia.

The diagnostic performance of the four models compares favorably with those presented in previous quantitative MBF studies (6,7,9). This is expected, as ambiguous cases have not been included in this data set. No significant differences in diagnostic performance were found between the models; however, the one-compartment model performed significantly worse than the Fermi model when it was evaluated with MPRs but not when it was evaluated in terms of stress MBF values. The one-compartment model is a less flexible parameterization of the response function than the Fermi model. It uses a monoexponential decay function, which is not able to model the early filling stage shoulder in the response function, which might limit accuracy or precision in the resulting MBF estimates. This is consistent with the observation that the variance of MPR measurements was largest with the one-compartment model.

The AHA standard mapping of myocardial segments to coronary artery territories performs poorly in individual patients because of the large anatomic variation in coronary blood supplies (23). This was apparent in our data set, where there was a substantial number of cases in which the minimum MBF perfusion segment did not map to the diseased coronary artery specified by the AHA mapping. The number of mismatches in our data agrees well with work comparing the AHA model directly with coronary territories assessed with MR angiography (29).

Figure 2

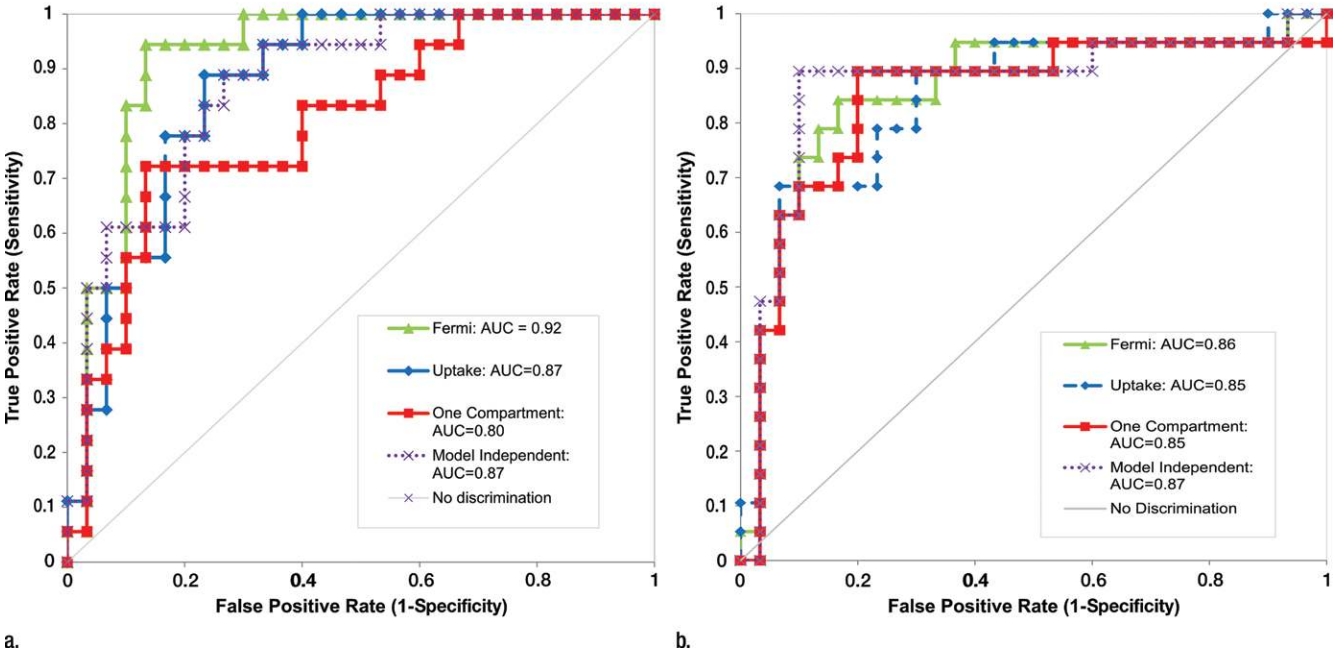

Figure 2: ROC curves show diagnostic performance of the four models using **(a)** MPR and **(b)** stress MBF as the diagnostic measure.

Table 3

Diagnostic Performance of the Four Models

Measurement	Fermi Method	Uptake Method	One-Compartment Model	Independent Deconvolution Model
Stress MBF				
AUC	0.86	0.85	0.85	0.87
ROC cut-off point (mL/min/g)	1.60	1.47	1.60	1.06
Sensitivity (%)	84.2 (16/19) [67.8, 100]	78.9 (15/19) [60.6, 97.3]	89.5 (17/19) [75.7, 100]	89.5 (17/19) [75.7, 100]
Specificity	83.3 (25/30) [70.0, 96.7]	76.7 (23/30) [61.5, 91.8]	80.0 (24/30) [65.7, 94.3]	90.0 (27/30) [79.3, 100]
MPR				
ROC AUC MPR	0.92	0.87	0.80	0.87
MPR ROC cut-off point (mL/min/g)	1.36	1.18	1.22	1.28
Sensitivity	94.4 (17/18) [83.9, 100]	88.9 (16/18) [74.4, 100]	72.2 (13/18) [51.5, 92.9]	83.3 (15/18) [66.1, 100]
Specificity	86.7 (26/30) [74.5, 98.8]	76.6 (23/30) [61.5, 91.8]	86.7 (26/30) [74.5, 98.8]	76.7 (23/30) [61.5, 91.8]

Note.—Data in parentheses are raw data. Data in brackets are 95% confidence intervals. Cutoff values are based on the perfusion measure used in the ROC analysis, which was the AHA segment with the lowest perfusion value.

No significant difference in diagnostic performance was found between the ROC curves generated by using stress MBF values and those generated by using MPRs. This is consistent with the findings of Huber et al (7). Our study findings enable us to confirm this observation in a larger data set. Our study does not address the use of rest imaging in the assessment of dark rim artifacts, which is important for visual assessment. However, when quantitative MBF estimates are to be used as the sole basis for diagnosis of ischemic heart disease, our results suggest that rest imaging can be removed from the imaging protocol, reducing the time of the investigation.

MBF values in patients without ischemia are comparable with those published in studies of healthy volunteers (10,15) and total exclusions were 6.5%, which compares favorably with the exclusion rate in other quantitative studies; for instance, Patel et al (9) excluded 23% of patients and Costa et al (6) excluded 16%.

Although excellent intermethod correlation was observed between the four methods, there were significant differences between average MBF measurements in most cases. The comparison of the Fermi model with

Figure 3

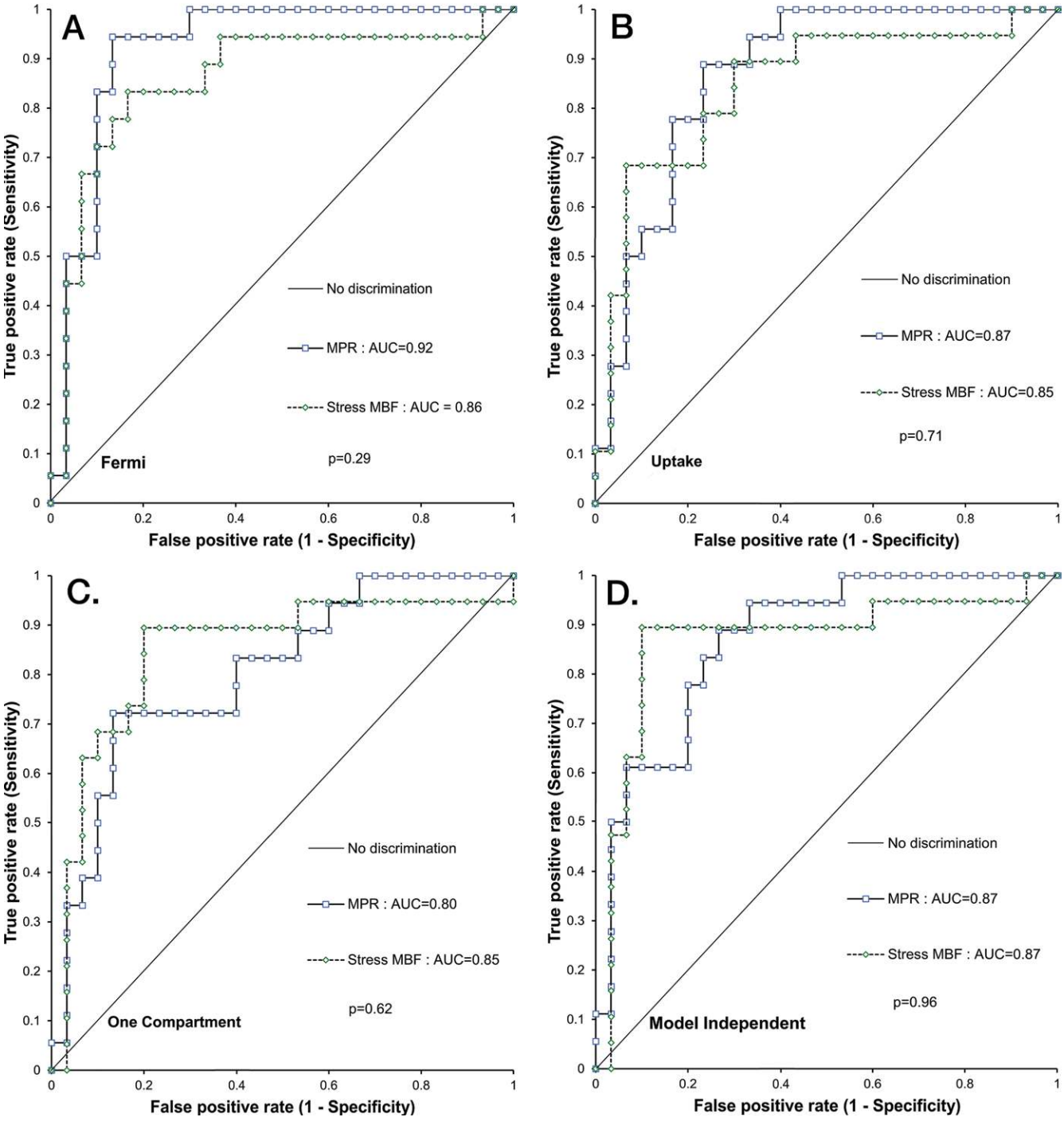

Figure 3: Direct comparison between MPR- and stress MBF–based ROC curves for, *A*, Fermi, *B*, uptake, *C*, one-compartment, and, *D*, model-independent deconvolution methods. DeLong et al ROC curve comparison *P* values are shown for each model on the relevant plot.

the one-compartment model did not follow this trend, as it showed no significant difference in MBF. Conversely, only the comparison of the Fermi model with the model-independent method showed a significant difference in MPR values. In a similar comparison study, Pack et al (12) only observed significant differences between only

Fermi-derived stress MBF values and other methods. The reason we saw differences where they did not may be due to the larger sample size in our study (50 subjects who underwent both rest and stress vs 20 patients who underwent rest and 14 who underwent stress [12]).

Bland-Altman assessment showed that the magnitude of the differences was small (stress MBF ≤0.48 mL/g/min and MPR ≤0.18). The uptake and model-independent methods generated systematically lower MBF estimates than did the Fermi and one-compartment methods. The uptake method requires early cropping of the data to avoid violating the in-flow only assumption, which could reduce MBF. Model-independent deconvolution is the least constrained method. Our implementation imposed smoothness by incorporating a first-order differential in the side constraint. This smooths the response function and can reduce flow estimates.

There were limitations of our study. This study used a matching diagnosis between SPECT and QCA to obtain the best reference standard available within the Clinical Evaluation of Magnetic Resonance Imaging in Coronary Heart Disease data set. The SPECT perfusion protocol was not performed with attenuation correction, which some have suggested may improve diagnostic accuracy (30), and higher spatial resolution measurements could have been achieved if PET imaging had been used. The study did not include a reference standard for quantitative MBF measurements, which could have been provided if PET measurements had been obtained. The lack of a completely linear arterial input function measurement, such as that acquired by using dual bolus (31) or dual sequence (32) data, was a limitation to this retrospective data set. It is important to note that the diagnostic accuracies achieved in this study are not representative of clinical diagnostic accuracy. Ambiguous cases, those in which QCA and SPECT measurements did not agree, were not included. This created a reliable reference standard for our comparison study; however, our results cannot be considered representative of clinical diagnostic performance. It is possible that there may be differences in the diagnostic power of the different methods that would only be apparent in these ambiguous cases, and this is a limitation of this study.

Practical application: The finding that all of the assessed methods perform equally well is important because the methods differ in complexity of implementation, in speed of computation, and in the amount of data required to quantify MBF. Simpler or quicker methods may be selected in the future without loss of diagnostic performance in quantitative studies. The practical implications of not performing a rest examination for quantitative studies has the potential to significantly reduce patient imaging time.

Disclosures of Conflicts of Interest: J.D.B. disclosed no relevant relationships. **D.R.M.** disclosed no relevant relationships. **S.P.S.** disclosed no relevant relationships. **S.P.** disclosed no relevant relationships. **J.P.G.** disclosed no relevant relationships. **A.R.** disclosed no relevant relationships.

References

1. Jaarsma C, Leiner T, Bekkers SC, et al. Diagnostic performance of noninvasive myocardial perfusion imaging using single-photon emission computed tomography, cardiac magnetic resonance, and positron emission tomography imaging for the detection of obstructive coronary artery disease: a meta-analysis. J Am Coll Cardiol 2012;59(19):1719–1728.
2. Christian TF, Rettmann DW, Aletras AH, et al. Absolute myocardial perfusion in canines measured by using dual-bolus first-pass MR imaging. Radiology 2004;232(3):677–684.
3. Kraitchman DL, Wilke N, Hexeberg E, et al. Myocardial perfusion and function in dogs with moderate coronary stenosis. Magn Reson Med 1996;35(5):771–780.
4. Ritter C, Brackertz A, Sandstede J, Beer M, Hahn D, Köstler H. Absolute quantification of myocardial perfusion under adenosine stress. Magn Reson Med 2006;56(4):844–849.
5. Fritz-Hansen T, Hove JD, Kofoed KF, Kelbaek H, Larsson HB. Quantification of MRI measured myocardial perfusion reserve in healthy humans: a comparison with positron emission tomography. J Magn Reson Imaging 2008;27(4):818–824.
6. Costa MA, Shoemaker S, Futamatsu H, et al. Quantitative magnetic resonance perfusion imaging detects anatomic and physiologic coronary artery disease as measured by coronary angiography and fractional flow reserve. J Am Coll Cardiol 2007;50(6):514–522.
7. Huber A, Sourbron S, Klauss V, et al. Magnetic resonance perfusion of the myocardium: semiquantitative and quantitative evaluation in comparison with coronary angiography and fractional flow reserve. Invest Radiol 2012;47(6):332–338.
8. Maredia N, Plein S, Younger JF, et al. Detection of triple vessel coronary artery disease by visual and quantitative first pass CMR myocardial perfusion imaging in the CE-MARC study [abstr]. J Cardiovasc Magn Reson 2011;13(Suppl 1):O29.
9. Patel AR, Antkowiak PF, Nandalur KR, et al. Assessment of advanced coronary artery disease: advantages of quantitative cardiac magnetic resonance perfusion analysis. J Am Coll Cardiol 2010;56(7):561–569.
10. Hsu L-Y, Rhoads KL, Holly JE, Kellman P, Aletras AH, Arai AE. Quantitative myocardial perfusion analysis with a dual-bolus contrast-enhanced first-pass MRI technique in humans. J Magn Reson Imaging 2006;23(3):315–322.
11. Zarinabad N, Chiribiri A, Hautvast GLTF, et al. Voxel-wise quantification of myocardial perfusion by cardiac magnetic resonance. Feasibility and methods comparison. Magn Reson Med 2012;68(6):1994–2004.
12. Pack NA, DiBella EV. Comparison of myocardial perfusion estimates from dynamic contrast-enhanced magnetic resonance imaging with four quantitative analysis methods. Magn Reson Med 2010;64(1):125–137.
13. Jerosch-Herold M, Wilke N, Stillman AE. Magnetic resonance quantification of the myocardial perfusion reserve with a Fermi function model for constrained deconvolution. Med Phys 1998;25(1):73–84.
14. Jerosch-Herold M, Swingen C, Seethamraju RT. Myocardial blood flow quantification with MRI by model-independent deconvolution. Med Phys 2002;29(5):886–897.
15. Pack NA, DiBella EV, Rust TC, et al. Estimating myocardial perfusion from dynamic contrast-enhanced CMR with a model-independent deconvolution method. J Cardiovasc Magn Reson 2008;10:52.
16. Vallée JP, Lazeyras F, Kasuboski L, et al. Quantification of myocardial perfusion with FAST sequence and Gd bolus in patients with

normal cardiac function. J Magn Reson Imaging 1999;9(2):197–203.

17. Vallée JP, Sostman HD, MacFall JR, et al. Quantification of myocardial perfusion by MRI after coronary occlusion. Magn Reson Med 1998;40(2):287–297.
18. Kurita T, Sakuma H, Onishi K, et al. Regional myocardial perfusion reserve determined using myocardial perfusion magnetic resonance imaging showed a direct correlation with coronary flow velocity reserve by Doppler flow wire. Eur Heart J 2009;30(4):444–452.
19. Ishida M, Ichihara T, Nagata M, et al. Quantification of myocardial blood flow using model based analysis of first-pass perfusion MRI: extraction fraction of Gd-DTPA varies with myocardial blood flow in human myocardium. Magn Reson Med 2011;66(5):1391–1399.
20. Ichihara T, Ishida M, Kitagawa K, et al. Quantitative analysis of first-pass contrast-enhanced myocardial perfusion MRI using a Patlak plot method and blood saturation correction. Magn Reson Med 2009;62(2):373–383.
21. Greenwood JP, Maredia N, Younger JF, et al. Cardiovascular magnetic resonance and single-photon emission computed tomography for diagnosis of coronary heart disease (CE-MARC): a prospective trial. Lancet 2012; 379(9814):453–460.
22. Greenwood JP, Maredia N, Radjenovic A, et al. Clinical evaluation of magnetic resonance imaging in coronary heart disease: the CE-MARC study. Trials 2009;10:62.
23. Cerqueira MD, Weissman NJ, Dilsizian V, et al. Standardized myocardial segmentation and nomenclature for tomographic imaging of the heart. A statement for healthcare professionals from the Cardiac Imaging Committee of the Council on Clinical Cardiology of the American Heart Association. Circulation 2002;105(4):539–542.
24. Cheong LH, Koh TS, Hou Z. An automatic approach for estimating bolus arrival time in dynamic contrast MRI using piecewise continuous regression models. Phys Med Biol 2003;48(5):N83–N88.
25. Fritsch F, Carlson R. Monotone piecewise cubic interpolation. SIAM J Numer Anal 1980;17(2):238–246.
26. Biglands J, Magee D, Boyle R, Larghat A, Plein S, Radjenović A. Evaluation of the effect of myocardial segmentation errors on myocardial blood flow estimates from DCE-MRI. Phys Med Biol 2011;56(8):2423–2443.
27. Broadbent DA, Biglands JD, Larghat A, et al. Myocardial blood flow at rest and stress measured with dynamic contrast-enhanced MRI: comparison of a distributed parameter model with a Fermi function model. Magn Reson Med 2013;70(6):1591–1597.
28. DeLong ER, DeLong DM, Clarke-Pearson DL. Comparing the areas under two or more correlated receiver operating characteristic curves: a nonparametric approach. Biometrics 1988;44(3):837–845.
29. Zakkaroff C, Radjenovic A, Biglands JD, Plein S, Greenwood JP, Magee DR. Registration of coronary MRA to DCE-MRI myocardial perfusion series improves diagnostic accuracy through the computation of patient-specific coronary supply territories: a CE-MARC sub-study [abstr]. J Cardiovasc Magn Reson 2014;16(Suppl 1):O25.
30. Masood Y, Liu Y, Depuey G, et al. Clinical validation of SPECT attenuation correction using x-ray computed tomography-derived attenuation maps: multicenter clinical trial with angiographic correlation. J Nucl Cardiol 2005;12:676–686.
31. Köstler H, Ritter C, Lipp M, Beer M, Hahn D, Sandstede J. Prebolus quantitative MR heart perfusion imaging. Magn Reson Med 2004;52(2):296–299.
32. Gatehouse PD, Elkington AG, Ablitt NA, Yang GZ, Pennell DJ, Firmin DN. Accurate assessment of the arterial input function during high-dose myocardial perfusion cardiovascular magnetic resonance. J Magn Reson Imaging 2004;20(1):39–45.